titanium surface by APTES silanization is an effective approach to prevent bacterial infection in vivo.
http://dx.doi.org/10.1016/j.jot.2016.06.038

131
IN VIVO EVALUATION OF THE ANTI-INFECTION POTENTIAL OF GENTAMICIN-LOADED NANOTUBES ON TITANIA IMPLANTS

Ying Yang, Tingting Tang
Shanghai Key Laboratory of Orthopaedic Implants, Department of Orthopedic Surgery, Shanghai Ninth People's Hospital, Shanghai, China

Introduction: Currently, implant-associated infection is one of the critical causes of implant failures in orthopedic surgery. Titanium and titanium alloys are the most widely used implant materials and have good biocompatibility and excellent mechanical properties. However, these implant surfaces also favor bacterial adhesion, colonization and biofilm formation, and there is competition of initial adhesion to the implant surface between bacteria and osteoprogenitors. Therefore, good antibacterial properties and osteoblast activity are the key points involved in implant material manufacturing.
Subjects and Methods: Thirty-six male Sprague-Dawley (SD) rats were used to establish an implant-associated infection model. A volume of 50 μl *Staphylococcus aureus* suspension (1×10^5 CFUs/ml) was injected into the medullary cavity of the left femur, and then the titanium rods without modification (Ti), titanium nanotubes without drug-loading (NT) and gentamicin-loaded titanium nanotubes (NT-G) were inserted with PBS-inoculated Ti rods as a blank control. X-ray images were obtained 1, 21, and 42 days after surgery, micro-CT, microbiological and histopathological analysis were used to evaluate the infections at the time of sacrifice.
Results: Radiographic signs of bone infection, including osteolysis, periosteal reaction, osteosclerosis and damaged articular surfaces were demonstrated in the infected Ti group and were slightly alleviated in the NT group, but not observed in the NT-G group. Meanwhile, the radiographic and gross bone pathological scores of the NT-G group were significantly lower than those of the infected Ti group (live bacterial growth compared with the Ti group; *p* confirmed decreased bacterial burden in the NT-G group compared with the Ti and NT groups).
Discussion and Conclusion: The traditional remedy of an infected implant is a prolonged systemic antibiotic administration after device removal. The local use of antibiotic-loaded nanotubes has been widely reported to prevent this intractable clinical condition experimentally. Meanwhile, nanostructured surface topographies have been explored as effective approaches for enhancing desirable osteogenesis. Our previous research has demonstrated that gentamicin-loaded nanotubes with diameters of 80 nm exhibited predictable drug release kinetics and significantly improved antimicrobial activity. In this study, we further investigated the effectiveness of gentamicin-loaded nanotubes on titanium surfaces to prevent implant-associated infections in a rat model. In general, this effective *in vivo* study showed that the NT-G group exhibited significant bacterial inhibition when compared with the Ti and NT groups in this *S. aureus* infection rat model. The NT coatings also resulted in alleviated bacterial burdens, and therefore demonstrated the feasibility of the clinical application of this antibiotic-loaded titanium nanotube-based implant for combating orthopedic implant-associated infection.
http://dx.doi.org/10.1016/j.jot.2016.06.039

132
A NOVEL FIXATIVE NEEDLE CARRIED Mg CAN PROMOTE FRACTURE HEALING IN OVX RATS

Yifeng Zhang
Nanjing University, Nanjing, China

Introduction: Magnesium (Mg) can promote the new bone formation in the periosteum region after intramedullary implanted into the rat femur canal. This osteogenic effect inspired us to apply it into the OVX rat fracture healing. Mg itself is too soft to fix the rat fracture bone directly, that puzzled clinicians without a resolution of enhancing Mg metal's strength. Here we designed a novel fixative needle-encapsulated Mg intramedullary nail to fixate the fractured bone. We speculated Mg ions which released through the window at middle site of the needle can promoted the fracture healing. That will make Mg's orthopedic application into an applicable real.
Methods: Three kinds of needle designs were drafted in software SolidWorks. Finite elemental analysis (FEA) was used to screen design drawing with the best mechanical performance and broad window area. 18G spinal needles were machined as rough blank. Mg degradation captured in designed needle was evaluated in vitro. 48 3-month old rats were ovariectomized and raised to 9-month old to perform osteoporosis. Then rats were made to closed fracture on right femur and fixed separately by designed needle ($n = 24$) and blank needle ($n = 24$). Samples were harvested at week 2, 4, 8, 12 (all groups with 6 samples at each time point). Micro-CT scanning and X-ray photographs were applied to analyse fracture callus. Samples at week 12 were under mechanical test. Callus area and length in X-ray results, callus total volume and bone volume, callus bone density, mechanical strength and E-modulus were analysed.
Results: The window design was evolved from original semi-roundness shape to the cruciatedly interlacing holes. However semi-roundness shape needle was broken in the rat femur fracture fixation at week 4 to 6. The ideal design preserved enough window area and strong enough to fixate the fracture bone. The window area in 1/5 needle outer diameter design was about 3.6 square millimeters, just 0.8 times to that of $^1/_2$ needle outer diameter design, but the strength was enforced significantly. The cruciatedly interlacing holes design was 18 holes interlacingly arranged in the middle site of the needle. Holes diameter was 0.5 mm. 18 holes distributed at needle surface with length of 10 mm. So sum area of total 18 holes was 3.53 square millimeters, it was closed to 1/5 needle outer diameter design. FEA results showed that both middle site and lateral site bearing were largest in needle with $^1/_2$ outer diameter design, the needle with 1/5 outer diameter design was less but still more than the intact needle. The needle with cruciatedly interlacing holes design had almost no difference with the intact needle, and this design was our first choice. In fracture, lateral X-ray radiographs showed that Mg treated group showed 1.89 times callus area than the control group, its callus width was 1.38 times than the control at week 2. At week 4, Mg treated group had 1.64 times callus area than the control group, and the callus width was still 1.38 times than the control. At week 8, Mg treated group still had 1.71 times callus area than the control group, and the callus width was 1.4 times than the control. All the differences were vanished at week 12. CT results of fracture callus showed that Mg treated fracture bone group performed significantly more total callus bone volume than the control group at week 2, 4 and 8. At week 2, the total callus bone volume of Mg treated group was 1.178 times than that of control group. At week 4, the total callus bone volume of Mg treated bone was 1.417 times than the control group. At week 8, the Mg treated group still had 1.318 times than the control. We observed that the callus total volume in Mg treated group was remarkably higher than the control group from beginning to the end, and the increasing range was achieved to the top at week 4, after week 4, the increasing amount was sloping to a low value at week 8. Also all the differences were disappeared at week 12. At week 12, we carried biomechanical test, the results showed that Mg treated fracture femur had better bending resisting strength than the control (about 27% improvement to the control).
Discussion: FEA analysis helped us choosing a most appropriate needle design to fixate rat fracture bone and carrying Mg. We successfully applied Mg to treat fracture healing by a novel needle. X-ray and micro-CT results suggested the Mg containing needle significantly enhanced fracture callus volume. Biomechanical testing results proved Mg containing needle had excellent performance in fracture healing. This work firstly designed a hollow needle which carried Mg in treatment of fracture repair, and made Mg's orthopedic usage to be an applicable real in clinical field.
Conclusion: Data were presented as mean ± standard deviation. A two-sided, non-paired t test was used to analyze all the data, differences were considered significant as $p < 0.05$.
http://dx.doi.org/10.1016/j.jot.2016.06.040

149
HYDROTHERMALLY CONVERTED MARINE CORAL SCAFFOLD PROMOTES SEGMENTAL BONE DEFECT HEALING IN RATS

Sien Lin [a,b,c], Wayne Yuk Wai Lee [a,c], Yuxin Sun [a,c], Liao Cui [b], David William Green [d], Gang Li [a,c]
[a]*The Chinese University of Hong Kong-Astronaut Centre of China (CUHK-ACC) Space Medicine Centre on Health Maintenance of Musculoskeletal System, Shenzhen Research Institute, The Chinese University of Hong Kong, Shenzhen, Guangdong, China*
[b]*Department of Pharmacology, Guangdong Key Laboratory for Research and Development of Natural Drugs, Guangdong Medical University, Zhanjiang, Guangdong, China*
[c]*Department of Orthopaedics and Traumatology, The Li Ka Shing Institute of Health Sciences, Faculty of Medicine, The Chinese University of Hong Kong, Hong Kong*
[d]*Biomedical and Tissue Engineering Research Group, Faculty of Dentistry, The University of Hong Kong, Hong Kong*

Objective: Large segmental bony defects remain tough problems in clinical setting. Concentrated efforts have being made to develop different materials that can mimic both function and structure of natural bone tissue. Bone tissue engineering approaches are becoming more effective alternatives to autologous or allogenic bone grafting in the orthopedic surgery. Marine coral showed great potential as bio-scaffolds for their biomimetic composition and structure. Physical or chemical fabrication can reduce their immunogenicity and increase the mechanical strength. This study aims to investigate the effects of hydrothermal converted coral biomaterials on cell viability and bone regeneration *in vitro* and in *vivo*.
Methods: Hydroxyapatite nanopartical-coated and hydrothermal converted coral scaffolds were fabricated using established protocols. Natural coral and β-tricalcium phosphate (β-TCP) were taken as controls. Micro-computed tomography

(CT) analysis was performed to determine the microstructure and porosity of the materials. The rat bone marrow-derived mesenchymal stem cells (MSCs) were seeded onto the scaffolds, the cell proliferation was determined using Alamar Blue cell viability assay. Surface of the materials were scanned by scanning electron microscope (SEM) before and after cell seeding. Segmental bone defects (3 mm*3 mm*2 mm) were made on the right femora of Sprague-Dawley rats under anesthesia and filled with β-TCP (n = 6), natural coral (n = 6), hydroxyapatite nanoparticle-coated coral (n = 6), or hydrothermal treated coral (n = 6), respectively. Samples were harvested for micro-CT and then decalcified for histology analysis after 8 weeks.
Results: Results of Micro-CT showed all the scaffolds exhibited a homogenous structure with interconnected open pores. The internal porosity of the four materials were 40–60%. Cell proliferation was significantly increased when MSCs were seeded onto the surface of hydrothermal treated coral scaffolds compared to other materials after 3 days. Results of SEM showed that a large number of MSCs attached well onto the surface of hydrothermal treated coral rather than other materials. In the animal study, there was no significant difference in the volume of mineralized tissue within the defect area in the four groups. The histological results showed significantly more bone formation in the femoral defect region in the group transplanted with hydrothermal treated coral scaffolds, indicating that bone formation was enhanced by the hydrothermal treated coral scaffolds.
Conclusion: Hydrothermal converted coral scaffolds showed superior repair effect in rat critical-sized femoral defect models, when compared with either β-TCP, natural coral, or hydroxyapatite nanopartical-coated coral. This may be a new biomaterial to be explored as bone substitute.
http://dx.doi.org/10.1016/j.jot.2016.06.041

170
SYNTHESIS, CHARACTERIZATION AND BIOLOGICAL EVALUATION OF STRONTIUM/MAGNESIUM-CO-SUBSTITUTED HYDROXYAPATITE

Zhen Geng [a], Renfeng Wang [c], Zhaoyang Li [a,b], Zhenduo Cui [a], Shengli Zhu [a,b], Yanqin Liang [a], YunDe Liu [c], Huijing Bao [c], Xue Li [c], Qianyu Huo [c], Zhili Liu [c], Xianjin Yang [a,b]
[a]*School of Materials Science and Engineering, Tianjin University, China*
[b]*Tianjin Key Laboratory of Composite and Functional Materials, China*
[c]*School of Laboratory Medicine, Tianjin Medical University, China*

The present study aims to investigate the contribution of two biologically important cations, Mg^{2+} and Sr^{2+}, when co-substituted into the structure of hydroxyapatite ($Ca_{10}(PO_4)_6(OH)_2$, HA). The substituted samples were synthesized by a hydrothermal method that involved the addition of Mg^{2+} and Sr^{2+} containing precursors to partially replace Ca^{2+} in the apatite structure. Four co-substituted HA samples with different concentrations of Mg^{2+} and Sr^{2+} ((Mg+Sr)/(Mg+Sr+Ca) = 30%) were investigated, and they were compared with pure HA. Experimental results showed that only a limited amount of Mg (Mg/(Mg+Ca+Sr) < 14%) could successfully substitute for Ca in HA. In addition, Mg substitution resulted in reduced crystallinity, thermal stability, and lattice parameters of HA. In contrast, Sr could fully substitute for Ca. Furthermore, the addition of Sr increased the lattice parameters of HA. Here, we obtained the cation leach liquor (CLL) by immersing the prepared samples in a culture medium for cell experiments. The *in vitro* study showed that 10Mg20Sr promoted better MG63 cell attachment, proliferation, and differentiation than HA. Thus, the presence of an appropriate proportion of Mg and Sr could play a significant role in the increased biocompatibility of HA.
http://dx.doi.org/10.1016/j.jot.2016.06.042

171
3D PRINTING OF OSTEOPROMOTIVE POLY(TRIMETHYLENE CARBONATE)-HYDROXYAPATITE IMPLANTS FOR BONE REGENERATION.

O. Guillaume [a], M. Geven [b], K. Kluge [a], U. Eberli [a], S. Zeiter [a], D. Grijpma [b], M. Alini [a], G. Richards [a], D. Eglin [a]
[a]*AO Research Institute Davos, AO Foundation, Davos, Switzerland*
[b]*Department of Biomaterials Science and Technology, University of Twente, Enschede, The Netherlands*

Introduction: Manufacturing polymer scaffolds with controlled internal structure and degradation using stereolithography, and with incorporation of osteoinductive ceramic has seldom been achieved. Poly(trimethylene carbonate) (PTMC) based resin loaded with nano-hydroxyapatite (nHA) were recently produced to create implants using stereolithography (SLA)[1]. In this study, 3D macroporous scaffolds were fabricated and their osteopromotive effect was characterized under *in vitro* and *in vivo* conditions.
Subjects and Methods: PTMC-methacrylate resin mixed with nHA at 0, 20 and 40% w/w were prepared and scaffolds with 500 μm pores were fabricated by SLA. Human bone marrow stromal cells (hMSCs) were seeded at 150 × 10^3 cells/scaffold and cultivated for 4 weeks in osteogenic media. At the end of the cultivation, cell proliferation and viability was assessed using DNA quantification and Live-and-Dead staining and collagen deposition was evaluated histologically using Safranin O Fast Green. Subsequently, *in vivo* experiment were conducted by creating 4 calvarial defects of 6 mm Ø on 8 rabbits (agreement 19A/2015) using Codman perforator device (DePuySynthes). After cleaning and washing, the defects were either left empty (control group) or PTMC and PTMC/nHA at 20 and 40% w/w scaffolds (Ø 6 mm × H 3.5 mm) were inserted in the cavities. Following 6 weeks of implantation, osseointegration was assessed by X-ray scan and by histology (Giemsa–Eosin staining).
Results: PTMC scaffolds without and with 20 and 40% of nHA were successfully fabricated using SLA (Figure 1A). *In vitro* study showed that hMSCs were able to proliferate similarly in all scaffolds (Figures 1B and 1C) and deposit collagen-rich matrix. Following implantation, microCT analyses revealed that the incorporation of 40% w/w of nHA in PTMC significantly increased the amount of bone formation in the porosity of the biomaterials (Figure 1, 6 weeks post-implantation), which was also confirmed histologically. Importantly, post-mortem injection of black India ink staining permitted to appreciate the intense vascularization occurring in the porous network of the scaffolds, which is a critical requirement for bone tissue engineering.

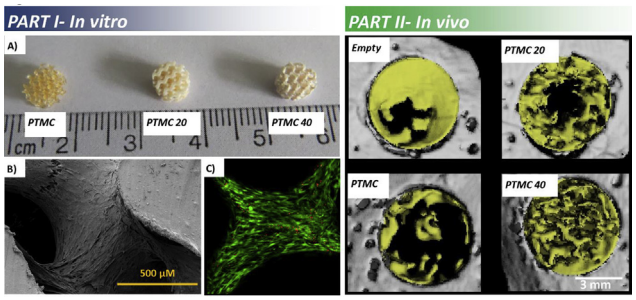

Figure 1 *In vitro and in vivo characterization of PTMC/nHA scaffolds* PART I-A) Macroscopic observation of the PTMC, PTMC 20 and PTMC 40% nHA scaffolds, and B) SEM and C) Live and Dead illustration of hBMSCs colonizing the scaffolds in vitro. PART II- MicroCT monitoring of neo-bone formation following 6 weeks of surgery for the empty defect (control group) compared to the different scaffolds (calvarial bone is coloured in grey and new bone tissue is coloured in yellow).

Discussion and Conclusion: For the first time, we reported the fabrication of PTMC/nHA-based SLA scaffolds for bone repair. We were able to endow PTMC biological activity by incorporating various amounts of nHA, allowing stimulation *in vivo* biomineralization.
Acknowledgements: NSFC-DG-RTD Joint Scheme (Project No. 51361130034) and the European Union's 7th Framework Program under grant agreement n° NMP3-SL-2013-604517.
References
[1] Geven MA et al. Fabrication of patient specific composite orbital floor implants by stereolithography. Polymers for Advanced Technologies 2015;26:1433–8.
http://dx.doi.org/10.1016/j.jot.2016.06.043

303
THE EFFECTS OF FIBER DIAMETER OF ELECTROSPUN PLLA SCAFFOLDS ON ANNULUS FIBROUS-DERIVED STEM CELLS

Pinghui Zhou [a], Feng Ling [a], Zhangqin Yuan [a], Bin Li [a,b]
[a]*Orthopedic Institute, Soochow University, Suzhou, China*
[b]*Department of Orthopaedic Surgery, The First Affiliated Hospital of Soochow University, Suzhou, China*

Background: Application of micro-/nanofibers as scaffold is a promising approach for annulus fibrous (AF) tissue engineering. However, it remains challenging because of heterogeneity of AF tissue in cellular, mechanical, and biochemical aspects. Previous studies have shown that the outer region of AF is rich in type I collagen and composed of larger fibers, while the inner region is rich in type II collagen and composed of smaller fibers. Therefore, mimicking the size of collagen fibers may be a feasible way for facilitating AF tissue reconstruction. In this study, we applied electrospinning technology to fabricate fibrous poly(L-lactic-acid) (PLLA) scaffolds of different fiber sizes and studied the effect of fiber diameter on the differentiation of annulus fibrous-derived stem cells (AFSCs).
Methods: PLLA fibrous scaffolds were fabricated using electrospinning technique and characterized through SEM, mechanical test and water contact angle measurement. After AFSCs were cultured on the scaffolds for 7 days, their morphology was examined using SEM and cytoskeleton staining. Expression of genes (Col-I, Col-II, Aggrecan) was quantified by RT-qPCR and the related proteins were analyzed by ELISA.
Results: PLLA fibrous scaffolds with three different fiber sizes were fabricated, of which the fiber diameter ranged from 3 μm to 8 μm. AFSCs proliferate well on all